

AperTO - Archivio Istituzionale Open Access dell'Università di Torino

Boson B Scattering at the LHCoson

This is the author's manuscript

Original Citation:

Availability:

This version is available <http://hdl.handle.net/2318/123077> since

Publisher:

SINP MSU

Terms of use:

Open Access

Anyone can freely access the full text of works made available as "Open Access". Works made available under a Creative Commons license can be used according to the terms and conditions of said license. Use of all other works requires consent of the right holder (author or publisher) if not exempted from copyright protection by the applicable law.

(Article begins on next page)

Boson-boson scattering at LHC

Elena Accomando, Alessandro Ballestrero, Aissa Belhouari and Ezio Maina ¹
INFN, Sezione di Torino and Dipartimento di Fisica Teorica, Università di Torino
Via P. Giuria 1, 10125, Torino, Italy

Abstract

We analyse some features of WW scattering processes at LHC. The severe cancellations between fusion diagrams and the other contributions evidence the necessity of complete calculations for studying the high WW invariant mass region and disentangling the standard Higgs case from new physics.

1 Introduction

Higgs discovery and Electroweak Symmetry Breaking (EWSB) studies are among the main purposes of LHC. The so-called boson-boson fusion process is one of the most promising Higgs production channels. If the Higgs mass is greater than 140 GeV, its main decay mode is in two W 's. The study of this channel requires a complete calculation of six fermion final states. On the other hand it is well known that a no-Higgs scenario would imply a violation at high energies of partial wave perturbative unitarity, which would manifest itself in particular in WW scattering processes. In this sense WW scattering processes hold the key of EWSB. Possible new physics, which should account for the restoration of unitarity, would manifest itself there. As it is experimentally impossible to measure WW scattering, there is great interest in studying at LHC processes of the type $PP \rightarrow qq'VV$ ($V = W, Z$), which contain boson-boson fusion diagrams. One expects that this contribution dominates in particular kinematical regions and that it is possible from these studies to gain a better understanding of EWSB.

In the following we consider some theoretical difficulties connected with this kind of physics and we argue that it is necessary a full control of all six fermion processes. Some of the results presented are obtained with PHASE[1], a new Monte Carlo and event generator aimed at this scope.

2 From six fermion final states to WW scattering

In order to study WW scattering effects, one has to explore six fermion final states at LHC. The situation is

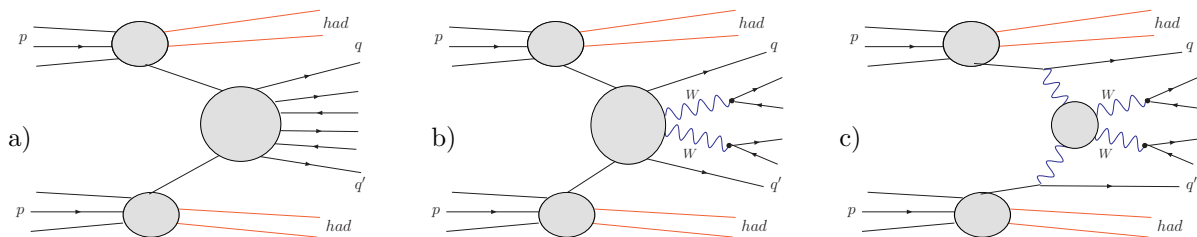


Figure 1: Representation of six fermion processes at LHC (a), $qq'WW$ production (b) and boson-boson scattering contributions (c).

depicted schematically in Fig. 1. Six fermion processes initiated by two partons (a), contain contributions from a set of diagrams with two decaying W 's (b). These in turn contain diagrams with two off shell bosons “emitted” by the incoming quarks which scatter to the final state W 's (c). These latter contributions are normally indicated as boson-boson fusion.

Ideally, informations on WW scattering should be deduced isolating the contributions of the diagrams of Fig. 1 (c), deconvoluting them from the pdf's of the incoming partons and extrapolating the

¹Talk given by A. Ballestrero.

Work supported by the European Union (EU) under contract HPRN-CT-2000-00149. The work of E.A. is supported by the MIUR under Contract “Rientro dei Cervelli” Decreto MIUR 26-01-2001 N. 13

WW scattering subdiagrams to on shell incoming W 's. This is a formidable task, and we will consider in the following some theoretical reasons why we believe that it cannot be accomplished as such. It seems however possible to find relevant differences between the Higgs and no-Higgs case, especially in distributions of the invariant mass of the two final W 's, which is the variable that in this context plays the role of the center of mass energy in the pure WW scattering process.

3 WW scattering and gauge invariance

Let us now consider the hard process $qq' \rightarrow qq'W^+W^-$. The corresponding Feynman diagrams can be classified in different topologies, as shown in Fig. 2.

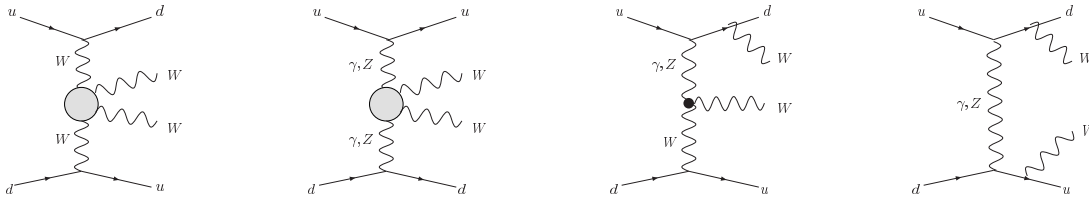


Figure 2: Different types of Feynman diagrams for the process $qq' \rightarrow qq'W^+W^-$

Essentially one has two contributions: boson-boson fusion (first two on the left) and all the rest in which at least one of the final W 's is emitted by fermion lines. Only the former belongs to Fig. 1 (c). The two sets are not separately gauge invariant and considering only one of them may be dangerous.

It is known since a long time[2] that there are large cancellations from negative interference between boson-boson fusion diagrams and the rest. We have analysed in detail such effects for the sample process $PP \rightarrow us \rightarrow dcW^+W^-$, in order to understand if one can find a particular gauge and a kinematical region in which the cancellations at LHC are not so severe. Some of our results are reported in Table 1 and in Figs 3,4.

no-Higgs	σ (pb)	ratio WW/all
all diagrams	1.86 E-2	
WW fusion (unitary gauge)	6.67	358
WW fusion (Feynman gauge)	0.245	13

Table 1: Cross sections for the process $PP \rightarrow us \rightarrow dcW^+W^-$ evaluated using all diagrams or only the WW fusion subset, and their ratio.

We find that, among the various R_ξ gauges, the Feynman gauge is the one which diminishes the interference. However, we see from Table 1 that even in this case the separate contributions of WW fusion and of the remaining diagrams have total cross sections an order of magnitude larger than the exact one, computed with all diagrams. The numbers reported in Table 1 refer to the no-Higgs case. For $M_H=200$ GeV in the region of invariant masses above the Higgs peak ($M_{WW} > 300$ GeV), the ratios are even larger, by about a factor of 2.

Considering now the distributions reported in Fig. 3, one realizes that the shape of the curve for total (left) and WW fusion only (right) is quite different and that the ratio between the two curves grows with the WW invariant mass. This effect is much more relevant in unitary gauge.

Fusion diagrams are expected to peak in the region of low momentum transfer from incoming quarks. Therefore we have analysed in Fig. 4 the double differential distributions $d\sigma/dt_1dt_2$ with $t_{1,2} = \sqrt{-(p_{u,s} - p_{d,c})^2}$ for the process $PP \rightarrow us \rightarrow dcW^+W^-$. Again the conclusion is that the WW fusion subset has a different behaviour compared with the complete calculation. The interference effects are non negligible even for moderate values of $t_{1,2}$ where the complete cross section is larger.

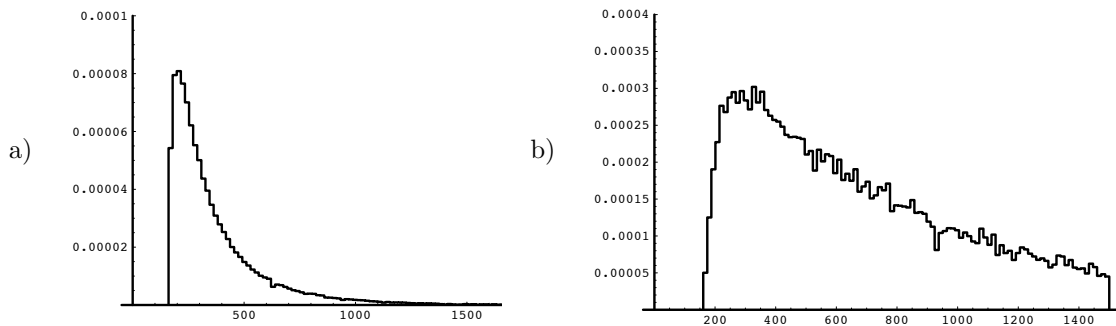


Figure 3: Distributions of $d\sigma/dM_{WW}$ (pb/GeV) for the process $PP \rightarrow us \rightarrow dcW^+W^-$, using all diagrams (a) or only the WW fusion subset in Feynman gauge (b).

The plots of Fig. 4 have been obtained excluding contributions from Higgs diagrams ($m_H \rightarrow \infty$ limit). The qualitative behaviour does not change if one includes them and excludes the region $M_{WW} \approx M_H$.

The Equivalent Vector Boson Approximation (EVBA) [3], which is gauge independent, is often used to estimate the contribution of the boson-boson fusion. The validity of such an approximation for massive vector bosons has been studied in the literature [4]. It appears that at LHC energies the EVBA is a reasonable approximation to the complete cross section for Higgs production but not for boson-boson invariant masses away from the peak. Moreover distributions such as those in fig 4 (a) cannot be correctly reproduced.

4 PHASE Monte Carlo

The strong cancellations examined in the previous section indicate that it is necessary to use complete calculations for the analysis of boson-boson physics. We believe that also considering qqWW final state and then decaying the W 's to 4 fermions is an approximation to the complete six fermion calculations that might not be sufficient for some analyses. We will give an example of this in the next section.

The first version of the new Monte Carlo and event generator PHASE [1] for six fermion final states has recently been completed. This is a Monte Carlo for LHC dedicated studies with full physics and detector simulation of boson-boson fusion and scattering, Higgs production in this channel, $t\bar{t}$ production, triple and quadruple boson couplings, three boson production.

The first version of PHASE can be used for processes with 4 quarks, a lepton and a neutrino in the final state. Processes are computed at $O(\alpha_{em}^6)$.

Matrix elements are evaluated with routines written with PHACT [5]. The number of different processes that can at present be computed is of the order of one thousand, each described by hundreds Feynman diagrams. The calculation is organized in such a way that only two groups of respectively 101 and 305 independent diagrams are recursively evaluated with a technique which makes repetitive use of subdiagrams to get a faster evaluation. PHASE adopts a new integration method which combines adaptive and multichannel strategies. High precision and efficiency has been obtained. PHASE can be used to evaluate any individual process or in the so called one-shot mode for generation[6]. In the latter, events of all processes or any subset can be generated at once in the right proportion, after the integrand maxima and phase space grids for the various processes have been computed in a preparatory run.

5 Boson-boson fusion and Higgs at high WW masses

In order to study in more detail the consequences of neglecting part of the calculations and to find out whether also in the complete calculations one can evidenciate differences between Higgs and no-Higgs case, we examine in this section the process $PP \rightarrow ud \rightarrow udc\bar{s}\mu\bar{\nu}_\mu$. One can select the resonant diagrams $PP \rightarrow ud \rightarrow udW^+W^- \rightarrow udc\bar{s}\mu\bar{\nu}_\mu$ and analyse the M_{WW} distributions. Moreover, even if the W 's are

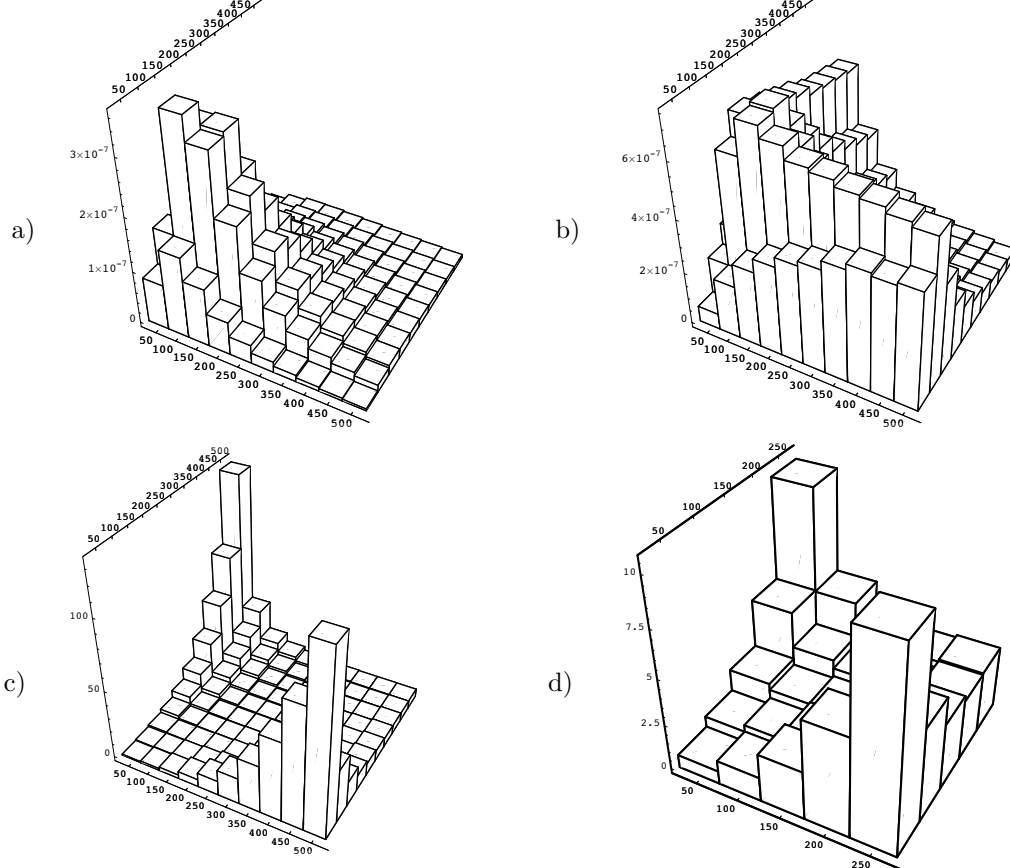


Figure 4: Double differential distributions of $d\sigma/dt_1 dt_2$ (pb/GeV^2) with $t_{1,2} = \sqrt{-(p_{u,s} - p_{d,c})^2}$ for the process $PP \rightarrow us \rightarrow dcW^+W^-$, using all diagrams (a) or only the WW fusion subset in Feynman gauge (b). The remaining plots represent the ratio WW/all as a function of t_1, t_2 for the total region (c) and for small t 's (d).

off shell, one can define and separate Longitudinal and Transverse final polarizations. We study in fig. 5 the M_{WW} distributions for the Unpolarized case (UN) and Longitudinal Longitudinal (LL) one. It is expected that EWSB effects manifest themselves in this distribution and that they are more pronounced for the LL case. We have imposed the following cuts:

$$1 < \eta(d) < 5.5 \quad -1 > \eta(u) > -5.5 \quad 70 < M(sc, \mu\nu) < 90 \text{ GeV}$$

$$E(u, d, c, s, \mu) > 20 \text{ GeV} \quad P_T(u, d, c, s, \mu) > 10 \text{ GeV}.$$

It is evident, from the first and third curve of fig. 5 from above, that considering only LL contributions underestimates the differential cross section by at least a factor ten. The exact ratio is strongly dependent on the Higgs mass.

In the other two curves we have required $p_T^W > M_W$. A cut of this kind is unavoidable if one uses the EVBA approximation, in order to keep under control the divergence of the on shell $WW \rightarrow WW$ diagram with γ exchange in t channel. One can see from the second and fourth curve from the top that in this case the difference between LL and UN is even larger.

In fig. 6 we study the differences between Higgs and no-Higgs ($m_H \rightarrow \infty$) scenarios for the full six fermion calculation and for the case in which only resonant $PP \rightarrow ud \rightarrow udW^+W^- \rightarrow udc\bar{s}\mu\bar{\nu}_\mu$ diagrams are used.

We plot the “reconstructed” WW mass. By this we mean the following: we select the most forward (f) and the most backward (b) jet, and call the remaining jets central (c). The invariant mass of the two central jets, the lepton and the neutrino, is what we call “reconstructed mass”. We impose the following cuts:

$$2 < \eta(j_f) < 6.5 \quad -2 > \eta(j_b) > -6.5 \quad |\eta(j_c, \mu)| < 3$$

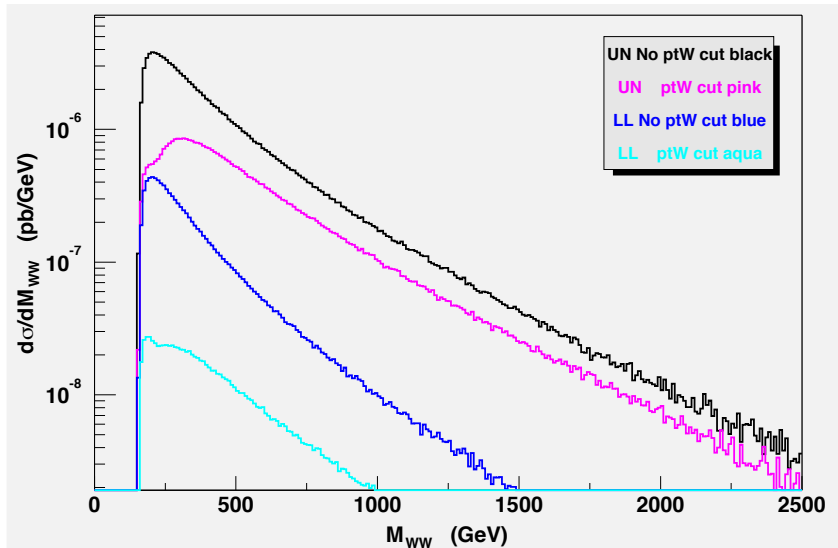


Figure 5: Differential distributions for the process $PP \rightarrow ud \rightarrow udW^+W^- \rightarrow udc\bar{s}\mu\bar{\nu}_\mu$ with $m_H = 120$ GeV for unpolarized and longitudinally polarized W's. Cuts are described in the text

$$E(j, \mu) > 20 \text{ GeV} \quad P_t(j, \mu) > 10 \text{ GeV} \quad M(jj) > 20 \text{ GeV} \\ |M(j_c, j_c) - M_W| < 20 \text{ GeV} \quad M_T(\mu\bar{\nu}_\mu) < M_W + 20 \text{ GeV},$$

One may notice from fig. 6 that the two upper curves, corresponding to only resonant diagrams, substantially differ in the high mass region from the complete calculation. It is even more important to outline that the two lower curves, describing the complete calculation for the Higgs and no-Higgs scenario, differ among themselves by a factor $\approx 2 \div 3$. This is encouraging with respect to the possibility of finding signals of EWSB at LHC.

6 Conclusions

We have found that the extraction of boson-boson scattering contributions at LHC can be problematic due to gauge invariance and cancellation effects. There are nevertheless clear indications that, if one uses the complete calculations and relies on appropriate cuts, which still have to be optimized, the Higgs and no-Higgs scenarios show appreciable differences. If a non SM EWSB mechanism is at work, much more dramatic phenomena would show up in boson-boson invariant mass distributions. We believe that a realistic study with all processes and full detector simulation is worthwhile and needed. PHASE has been developed to this end.

Acknowledgments

A. Ballestrero is grateful to all the organizers of QFTHEP04 for the pleasant and constructive atmosphere during the workshop and for the warm hospitality.

References

- [1] E. Accomando, A. Ballestrero and E. Maina, Nucl. Instrum. Meth. A534 (2004) 265
- [2] R. Kleiss and J.W. Stirling, Phys. Lett. 182B (1986) 75
- [3] S. Dawson, Nucl.Phys. B249 (1985) 42; G.L. Kane, W.W. Repko and W.B. Rolnick, Phys.Lett. 148B (1984) 367; J. Lindfors, Z. Phys. C28 (1985) 427

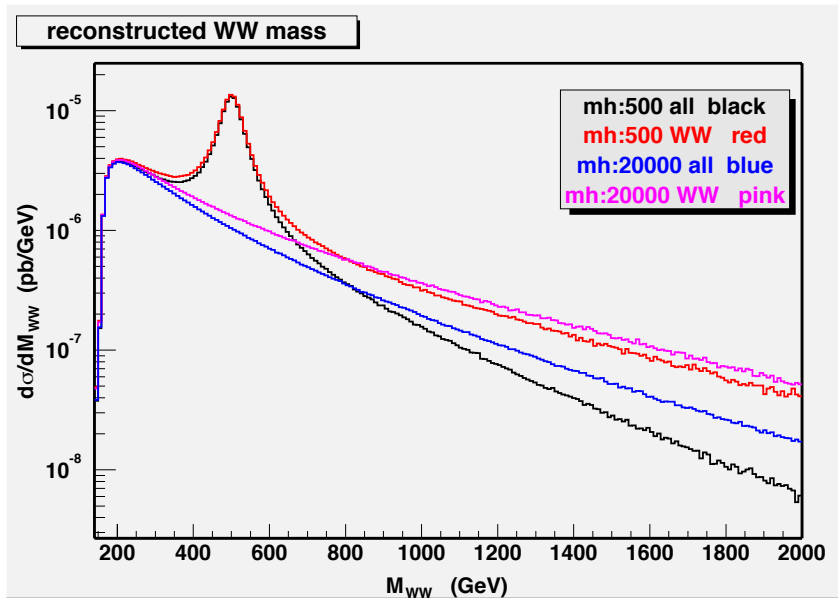


Figure 6: Reconstructed WW mass distributions for the process $PP \rightarrow ud \rightarrow udc\bar{s}\mu\bar{\nu}_\mu$ in the Higgs and no-Higgs ($m_H \rightarrow \infty$) case, with the full set and WW resonant only diagrams. Cuts are defined in the text.

- [4] I. Kuss and H. Spiesberger, Phys.Rev. D53 (1996) 6078; M. Chanowitz and M.K. Gaillard, Nucl.Phys. B261 (1985) 379; J.F. Gunion, J. Kalinowski and A. Tofighi-Niaki, Phys.Rev.Lett. 57 (1986) 2351; A. Abbasandi, W.W. Repko, D.A. Dicus and R. Vega, Phys.Rev. D38 (1988) 2770
- [5] A. Ballestrero, hep-ph/9911318, in: Proceedings of XIVth Int. Workshop on High Energy Physics and Quantum Field Theory (QFTHEP'99) ed.by B.B. Levchenko and V.I. Savrin, p.303; A. Ballestrero and E. Maina, Phys.Lett. B350 (1995) 225
- [6] E. Accomando, A. Ballestrero and E. Maina, Comput Phys. Commun. 150 (2003) 166